

Analytic Relations for Magnifications and Time Delays in Gravitational Lenses with Fold and Cusp Configurations

Arthur B. Congdon¹, Charles R. Keeton¹ and C. Erik Nordgren²

¹*Department of Physics and Astronomy, Rutgers University, 136 Frelinghuysen Road, Piscataway, NJ 08854 USA;*
acongdon, keeton@physics.rutgers.edu

²*nordgren@sas.upenn.edu*

19 August 2021

ABSTRACT

Gravitational lensing provides a unique and powerful probe of the mass distributions of distant galaxies. Four-image lens systems with fold and cusp configurations have two or three bright images near a critical point. Within the framework of singularity theory, we derive analytic relations that are satisfied for a light source that lies a small but finite distance from the astroid caustic of a four-image lens. Using a perturbative expansion of the image positions, we show that the time delay between the close pair of images in a fold lens scales with the cube of the image separation, with a constant of proportionality that depends on a particular third derivative of the lens potential. We also apply our formalism to cusp lenses, where we develop perturbative expressions for the image positions, magnifications and time delays of the images in a cusp triplet. Some of these results were derived previously for a source asymptotically close to a cusp point, but using a simplified form of the lens equation whose validity may be in doubt for sources that lie at astrophysically relevant distances from the caustic. Along with the work of Keeton et al. (2005), this paper demonstrates that perturbation theory plays an important role in theoretical lensing studies.

Key words: gravitational lensing – cosmology: dark matter – cosmology: theory – galaxies: structure – methods: analytical

1 INTRODUCTION

Gravitational lensing, or the bending of light by gravity, offers an exciting synergy between mathematics and astrophysics. Singularity theory provides a powerful way to describe lensing near critical points (Schneider et al. 1992; Petters et al. 2001), which turns out to have important implications for astrophysics and the quest to understand dark matter. Four-image lensed quasars can be broadly classified, according to image geometry, as either folds, cusps or crosses. We are interested in folds and cusps, which occur when the light source is close to the caustic curve, along which the lensing magnification is infinite (see top row of Fig. 1). Fold lenses feature a close pair of bright images, while cusp lenses have a close triplet of bright images (see bottom row of Fig. 1). By expanding the gravitational potential of the lens galaxy in a Taylor series, one finds that the image magnifications satisfy simple analytic relations, viz.

$$|\mu_A| - |\mu_B| \approx 0 \quad \text{and} \quad |\mu_A| - |\mu_B| + |\mu_C| \approx 0 \quad (1)$$

for fold pairs and cusp triplets, respectively (Blandford & Narayan 1986; Mao 1992; Schneider & Weiss 1992; Schneider et al. 1992; Zahkarov 1995; Gaudi & Petters 2002a,b; Keeton et al. 2003, 2005). For a fold pair, the two images have opposite parity, hence the negative sign. For a cusp triplet, the middle image (B) has opposite parity from the outer images (A and C). Note that in practice, one works with the image fluxes, which are directly observable, rather than the magnifications, which are not. This leads to the equivalent relations:

$$R_{\text{fold}} \equiv \frac{F_A - F_B}{F_A + F_B} \approx 0 \quad \text{and} \quad R_{\text{cusp}} \equiv \frac{F_A - F_B + F_C}{F_A + F_B + F_C} \approx 0, \quad (2)$$

where the image flux F_i is related to the source flux F_0 by $F_i = |\mu_i|F_0$.

Observationally, the fold and cusp relations are violated in several lens systems (e.g., Hogg & Blandford 1994; Falco et al. 1997; Keeton et al. 1997, 2003, 2005). These so-called “flux-ratio anomalies” are taken as strong evidence that lens galaxies contain significant small-scale structure (e.g., Mao & Schneider 1998; Metcalf & Madau 2001; Chiba 2002). Since global modifications of the lens potential (modeled with multipole terms, for example) cannot explain the anomalous flux ratios (Evans & Witt 2003; Congdon & Keeton 2005; Yoo et al. 2005, 2006), it is generally believed that lens galaxies must contain substructure in the form of mass clumps on a scale $\gtrsim 10^6 M_\odot$ (Dobler & Keeton 2006). Indeed, substructure is observed in at least two lens systems, in the form of a dwarf galaxy near the main lens galaxy (Schechter & Moore 1993; McKean et al. 2007). The substructure could well be invisible, though; numerical simulations of structure formation in the cold dark matter (CDM) paradigm predict that galaxy dark matter halos are filled with hundreds of dark subhalos (e.g., Klypin et al. 1999; Moore et al. 1999). The abundance of flux-ratio anomalies in lensed radio sources implies that lens galaxies contain $\sim 2\%$ (0.6–7% at 90% confidence) of their mass in substructure (Dalal & Kochanek 2002). This may be somewhat higher than the amount of CDM substructure (e.g., Mao et al. 2004), although new higher-resolution simulations are attempting to refine the theoretical predictions and make more direct comparisons with lensing observations (e.g., Gao et al. 2004; Strigari et al. 2007; Diemand et al. 2007). While there is still work to be done along these lines, it is clear that violations of the ideal fold and cusp relations provide important constraints on the small-scale distribution of matter in distant lens galaxies.

Keeton et al. (2003, 2005) pointed out that the ideal fold and cusp relations only hold for a source asymptotically close to the caustic. If we want to use flux-ratio anomalies to study small-scale structure in lens galaxies, it is vital that we understand how much R_{fold} and R_{cusp} can deviate from zero for realistic smooth lenses just because the source lies a small but finite distance from the caustic. To that end, Keeton et al. (2003) used a Taylor series approach to demonstrate that $R_{\text{cusp}} = 0$ to lowest order, and used Monte Carlo simulations to suggest that $R_{\text{cusp}} \propto d^2$, where d is the distance between the two most widely separated cusp images. In order to derive the leading non-vanishing term in R_{cusp} analytically, it would be necessary to extend the Taylor series to a higher order of approximation. This has not been done before, since including higher-order terms substantially complicates the analysis. Instead, previous authors have made assumptions about which terms are important and which terms can be neglected, in order to obtain an analytically manageable problem.

As we shall see, perturbation theory provides a natural way to overcome the difficulties of the Taylor series approach. Keeton et al. (2005) used perturbation theory to show that for fold lenses, R_{fold} is proportional to the image separation d_1 of the fold pair. We extend their analysis in several important ways. We derive the leading-order non-vanishing expression for R_{cusp} using perturbation theory. We also show, for the first time, how the combination of singularity theory and perturbation theory can be used to study *time delays* between lensed images for both fold and cusp systems. Working in analogy to flux ratios, we derive time-delay relations for fold and cusp lenses, which we will apply (in a forthcoming paper) to observed lenses in order to identify “time-delay anomalies.” As time delays join flux ratios in probing small-scale structure in lens galaxies (see Keeton & Moustakas 2008), singularity theory and perturbation theory once again provide the rigorous mathematical foundation.

2 MATHEMATICAL PRELIMINARIES

To study lensing of a source near a caustic, it is convenient to work in coordinates centered at a point on the caustic. Nonspherical lenses typically have two caustics. The “radial” caustic separates regions in the source plane for which one (outside) and two (inside) images are produced.¹ Within the radial caustic is the “tangential” caustic or astroid, which separates regions in the source plane for which two (between the two caustics) and four (inside the astroid) images are produced. We are interested in four-image lenses, where the source is within the astroid. We therefore make no further reference to the radial caustic. A typical astroid is shown in Figure 1 for a lens galaxy modeled by a singular isothermal ellipsoid (SIE), which is commonly used in the literature (e.g., Kormann et al. 1994) and appears to be quite a good model for real lens galaxies (e.g., Rusin & Kochanek 2005; Koopmans et al. 2006). It is customary to define source-plane coordinates (y_1, y_2) centered on the caustic and aligned with its symmetry axes. However, for fold and cusp configurations, where the source is a small distance from the caustic, it is more natural to work in coordinates (u_1, u_2) centered on the fold or cusp point. For convenience, we define the u_1 axis tangent to (and the u_2 axis orthogonal to) the caustic at that point. Transforming from the (y_1, y_2) plane to the (u_1, u_2) plane requires a translation plus a rotation. To derive this coordinate transformation, we follow the discussion in Appendix A1 in Keeton et al. (2005), which summarizes the results of Petters et al. (2001).

We begin by considering the lens equation $\mathbf{y} = \mathbf{x} - \nabla\psi(\mathbf{x})$, which maps the image plane to the source plane. The solutions to this equation give the image positions $\mathbf{x} \equiv (x_1, x_2)$ corresponding to a given source position $\mathbf{y} \equiv (y_1, y_2)$. The function $\psi(\mathbf{x})$ is the scaled gravitational potential of the lens galaxy projected onto the lens plane. A caustic is a curve along which the magnification is infinite, i.e., $\det(\partial\mathbf{y}/\partial\mathbf{x}) = \mu^{-1} = 0$, where $\partial\mathbf{y}/\partial\mathbf{x}$ is the Jacobian of \mathbf{y} , and is known as the inverse

¹ We are neglecting faint images predicted to form near the centers of lens galaxies, because they are highly demagnified and difficult to detect.

magnification matrix. We choose coordinates such that the origin of the source plane ($\mathbf{y} = 0$) is on the caustic. In addition, we require that the origin of the lens plane ($\mathbf{x} = 0$) maps to the origin of the source plane. We are interested in sources that lie near the caustic point ($\mathbf{y} = 0$), which give rise to lensed images near the critical point ($\mathbf{x} = 0$). In this case, we may expand the lens potential in a Taylor series about the point $\mathbf{x} = 0$. We then find that the inverse magnification matrix at $\mathbf{x} = 0$ is given by

$$\left. \frac{\partial \mathbf{y}}{\partial \mathbf{x}} \right|_0 = \begin{bmatrix} 1 - 2\hat{a} & -\hat{b} \\ -\hat{b} & 1 - 2\hat{c} \end{bmatrix}, \quad (3)$$

where

$$\hat{a} = \frac{1}{2}\psi_{11}(0), \quad \hat{b} = \psi_{12}(0), \quad \hat{c} = \frac{1}{2}\psi_{22}(0). \quad (4)$$

The subscripts indicate partial derivatives of ψ with respect to \mathbf{x} . Note that ψ has no linear part (since $\mathbf{y} = 0$ when $\mathbf{x} = 0$). For $\mathbf{y} = 0$ to be a caustic point, we must have $(1 - 2\hat{a})(1 - 2\hat{c}) - \hat{b}^2 = 0$. In addition, at least one of $(1 - 2\hat{a})$, $(1 - 2\hat{c})$, and \hat{b}^2 must be non-zero (Petters et al. 2001, p. 349). Consequently, $(1 - 2\hat{a})$ and $(1 - 2\hat{c})$ cannot both vanish. Without loss of generality, we assume that $1 - 2\hat{a} \neq 0$.

We now introduce the orthogonal matrix (see Petters et al. 2001, p. 344)

$$\mathbf{M} = \frac{1}{\sqrt{(1 - 2\hat{a})^2 + \hat{b}^2}} \begin{bmatrix} 1 - 2\hat{a} & -\hat{b} \\ \hat{b} & 1 - 2\hat{a} \end{bmatrix}, \quad (5)$$

which diagonalizes $\partial \mathbf{y} / \partial \mathbf{x}|_0$. We then define new orthogonal coordinates by

$$\boldsymbol{\theta} \equiv (\theta_1, \theta_2) \equiv \mathbf{M} \mathbf{x}, \quad \mathbf{u} \equiv (u_1, u_2) \equiv \mathbf{M} \mathbf{y}. \quad (6)$$

Note that the coordinate changes are the *same* in the lens and source planes. The advantage of using the same transformation in both the lens and source planes is that the lens equation takes the simple form

$$\mathbf{u} = \boldsymbol{\theta} - \nabla \psi(\boldsymbol{\theta}), \quad (7)$$

and that the inverse magnification can be written as

$$\mu^{-1} = \det \left(\frac{\partial \mathbf{u}}{\partial \boldsymbol{\theta}} \right). \quad (8)$$

The old and new coordinate systems in the source and image planes are shown in Figure 1. Since the caustic in the source plane maps to the critical curve in the image plane, the origin of the (θ_1, θ_2) frame is determined from that of the (u_1, u_2) frame. The orientation of the (θ_1, θ_2) axes is determined by the matrix \mathbf{M} , and is not necessarily related to the tangent to the critical curve.

Using the local orthogonal coordinates \mathbf{u} and $\boldsymbol{\theta}$, Petters et al. (2001, p. 346) showed that $\mathbf{x} = 0$ is a fold critical point if and only if the following conditions hold

$$(1 - 2\hat{a})(1 - 2\hat{c}) = \hat{b}^2, \quad 1 - 2\hat{a} \neq 0, \quad \psi_{222}(0) \neq 0. \quad (9)$$

For a cusp, the third condition above is replaced by the requirements that

$$\psi_{222}(0) = 0, \quad \psi_{122}(0) \neq 0, \quad \psi_{2222}(0) \neq 0. \quad (10)$$

Note in particular that $\psi_{222}(0) = 0$ for a cusp while $\psi_{222}(0) \neq 0$ for a fold; this indicates that these two cases must be treated separately.

We are interested in obtaining the positions, magnifications and time delays of images near critical points. Since these quantities depend only on the behavior of the lens potential near a fold or cusp point, we can expand $\psi(\boldsymbol{\theta})$ in a Taylor series about the point $\boldsymbol{\theta} = 0$. To obtain all the quantities of interest to leading order, we must expand the lens potential to fourth order in $\boldsymbol{\theta}$ (Petters et al. 2001, pp. 346–347):

$$\psi(\theta_1, \theta_2) = \frac{1}{2}(1 - K)\theta_1^2 + \frac{1}{2}\theta_2^2 + e\theta_1^3 + f\theta_1^2\theta_2 + g\theta_1\theta_2^2 + h\theta_2^3 + k\theta_1^4 + m\theta_1^3\theta_2 + n\theta_1^2\theta_2^2 + p\theta_1\theta_2^3 + r\theta_2^4, \quad (11)$$

where the coefficients $\{K, e, f, g, \dots, r\}$ are partial derivatives of the potential evaluated at the origin. Lensing observables are independent of a constant term in the potential, so we have not included one. Since $\boldsymbol{\theta} = 0$ maps to $\mathbf{u} = 0$, any linear terms in the potential must vanish. In the second order terms, the coefficients of the $\theta_1\theta_2$ and θ_2^2 terms are set to 0 and 1/2, respectively, in order to ensure that the point $\boldsymbol{\theta} = 0$ is a critical point (see Appendix A1 of Keeton et al. 2005).

3 THE FOLD CASE

In this section, we use perturbation theory (e.g., Bellman 1966) to derive an analytic relation between the time delays in a fold pair. To derive this expression, we must first obtain the image positions at which the time delay is evaluated. These

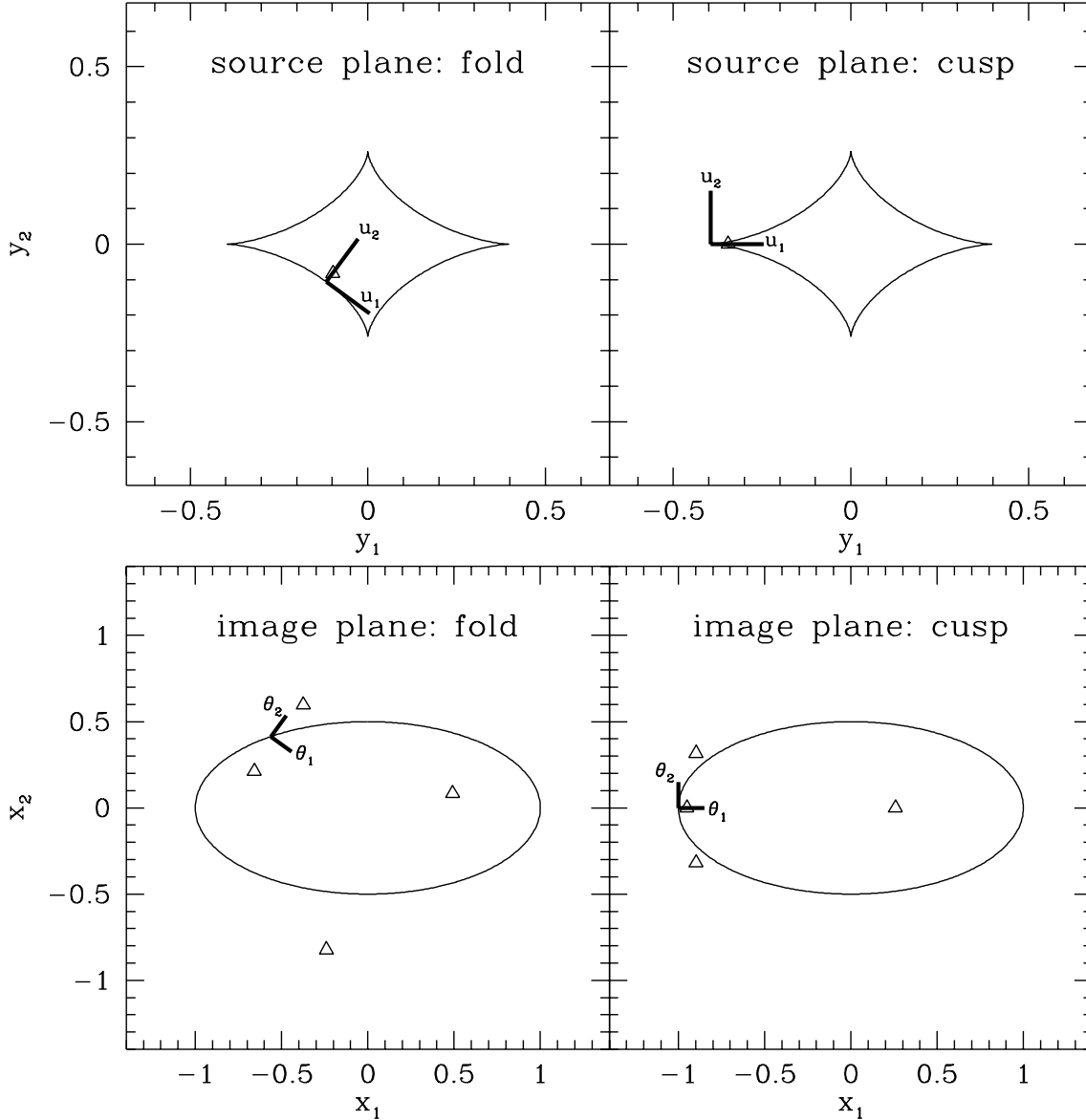


Figure 1. The curves show the caustic (top) and critical curve (bottom) for a singular isothermal ellipsoid (SIE) lens with minor-to-major axis ratio $q = 0.5$. The local orthogonal coordinates defined by the rotation matrix \mathbf{M} are indicated for a fold point (left) and a cusp point (right). In the top two panels, a source (triangle) with position (y_1, y_2) measured from the center of the caustic (astroid) has position (u_1, u_2) in the rotated coordinates centered on a fold point (left panel) or a cusp (right panel). In the bottom two panels, the four images (triangles) have positions (x_1, x_2) measured from the center of the critical curve (ellipse) and positions (θ_1, θ_2) in the rotated coordinates.

results were derived by Keeton et al. (2005). We offer a summary of their analysis in Section 3.1 and present our new results for the time delay in Section 3.2.

3.1 Image Positions

Since we are considering a source near a fold point, we write its position in terms of a scalar parameter ϵ , which we take to be small but finite. In particular, let $\mathbf{u} \rightarrow \epsilon \mathbf{u}$. Combining equations (7) and (11) we can write the lens equation as

$$\epsilon u_1 = K \theta_1 - (3e \theta_1^2 + 2f \theta_1 \theta_2 + g \theta_2^2) - (4k \theta_1^3 + 3m \theta_1^2 \theta_2 + 2n \theta_1 \theta_2^2 + p \theta_2^3), \quad (12)$$

$$\epsilon u_2 = -(f \theta_1^2 + 2g \theta_1 \theta_2 + 3h \theta_2^2) - (m \theta_1^3 + 2n \theta_1^2 \theta_2 + 3p \theta_1 \theta_2^2 + 4r \theta_2^3) \quad (13)$$

(see Petters et al. 2001, Theorem 9.1). To find the image positions, we expand θ_1 and θ_2 in a power series in ϵ . Since the left-hand sides of equations (12) and (13) are accurate to $\mathcal{O}(\epsilon)$, the right-hand sides must be accurate to the same order. Noting that the lowest-order terms on the right-hand side are linear or quadratic in θ , we write

$$\theta_1 = \alpha_1 \epsilon^{1/2} + \beta_1 \epsilon + \mathcal{O}(\epsilon)^{3/2}, \quad (14)$$

$$\theta_2 = \alpha_2 \epsilon^{1/2} + \beta_2 \epsilon + \mathcal{O}(\epsilon)^{3/2}. \quad (15)$$

Substituting into the lens equation, we obtain

$$0 = (\alpha_1 K) \epsilon^{1/2} - (3\alpha_1^2 e + 2\alpha_1 \alpha_2 f + \alpha_2^2 g - \beta_1 K + u_1) \epsilon + \mathcal{O}(\epsilon)^{3/2}, \quad (16)$$

$$0 = -(\alpha_1^2 f + 2\alpha_1 \alpha_2 g + 3\alpha_2^2 h + u_2) \epsilon - [2\alpha_1 \beta_1 f + 2(\alpha_1 \beta_2 + \alpha_2 \beta_1) g + 6\alpha_2 \beta_2 h + \alpha_1^3 m + 2\alpha_1^2 \alpha_2 n + 3\alpha_1 \alpha_2^2 p + 4\alpha_2^3 r] \epsilon^{3/2} + \mathcal{O}(\epsilon)^2. \quad (17)$$

Note that these equations are carried to different orders in ϵ , since the leading-order term in equation (12) is linear in θ , while the leading-order term in equation (13) is quadratic in θ .

Since ϵ is non-zero, equations (16) and (17) must be satisfied at each order in ϵ . We can work term by term to solve for the coefficients α_1 , α_2 and β_2 , and then write the image positions as

$$\theta_1^\pm = \frac{3hu_1 - gu_2}{3hK} \epsilon + \mathcal{O}(\epsilon)^{3/2}, \quad (18)$$

$$\theta_2^\pm = \pm \sqrt{\frac{-u_2}{3h}} \epsilon^{1/2} - \frac{3ghu_1 - g^2 u_2}{9h^2 K} \epsilon + \mathcal{O}(\epsilon)^{3/2}, \quad (19)$$

where the \pm labels indicate the parities of the images. From these equations, we see that two images form near the point $\theta = 0$ on the critical curve, provided that $(-u_2/3h) > 0$. Since $h \leq 0$ for standard lens potentials (e.g., an isothermal ellipsoid or isothermal sphere with shear), we must have $u_2 > 0$. In other words, the source must lie inside the caustic in order to produce a pair of fold images. In practice, a more useful quantity is the image separation, given by

$$d_1 = \sqrt{\frac{-4u_2}{3h}} \epsilon^{1/2} + \mathcal{O}(\epsilon)^{3/2}. \quad (20)$$

3.2 Time Delays

To find the time delay between the two fold images, we begin with the general expression for the scaled time delay (e.g., Schneider et al. 1992):

$$\hat{\tau}(\theta) \equiv \frac{\tau(\theta)}{\tau_0} = \frac{1}{2} |\theta - \mathbf{u}|^2 - \psi(\theta). \quad (21)$$

The scale factor is given by

$$\tau_0 = \frac{1 + z_L}{c} \frac{D_L D_S}{D_{LS}}, \quad (22)$$

where D_L , D_S and D_{LS} are the angular-diameter distances from the observer to lens, observer to source, and lens to source, respectively. The lens redshift is denoted by z_L . Making the substitution $\mathbf{u} \rightarrow (\epsilon u_1, \epsilon u_2)$, we have for the two fold images

$$\hat{\tau}_- \equiv \hat{\tau}(\theta_-) = \sqrt{-\frac{4}{27h}} (\epsilon u_2)^{3/2} + \mathcal{O}(\epsilon)^2, \quad (23)$$

$$\hat{\tau}_+ \equiv \hat{\tau}(\theta_+) = -\sqrt{-\frac{4}{27h}} (\epsilon u_2)^{3/2} + \mathcal{O}(\epsilon)^2. \quad (24)$$

The time delay between images is then (cf. Schneider et al. 1992, pp 190 - 191)

$$\Delta \hat{\tau}_{\text{fold}} \equiv \hat{\tau}_- - \hat{\tau}_+ = \sqrt{-\frac{16}{27h}} (\epsilon u_2)^{3/2} + \mathcal{O}(\epsilon)^2 = -\frac{h}{2} d_1^3 + \mathcal{O}(\epsilon)^2, \quad (25)$$

which is positive, in agreement with the general result that images with negative parity trail those with positive parity. We find that the only coefficient from the lens potential that enters the expression for the differential time delay is the parameter $h = \psi_{222}(0)/6$. We also see that to leading order in ϵ , the image separation and the differential time delay depend only on the u_2 component of the source position. Unlike the image positions, our expression for the time delay does not involve any of the fourth-order terms in the potential. This is because the time delay involves the potential directly, while the image positions depend on first derivatives of the potential. This means that all fourth-order terms in the potential enter the time delay at $\mathcal{O}(\epsilon)^2$, while these same terms enter at $\mathcal{O}(\epsilon)^{3/2}$ in quantities involving derivatives.

To summarize, $\Delta\hat{\tau}_{\text{fold}} \propto (\epsilon u_2)^{3/2} \propto d_1^3$. For comparison, $R_{\text{fold}} \propto d_1$. Since d_1 is small, a violation of the ideal relation $\Delta\hat{\tau}_{\text{fold}} = 0$ is more likely to indicate the presence of small-scale structure in the lens galaxy than would be indicated by a non-zero value of R_{fold} .

Our analytic expression for $\Delta\hat{\tau}_{\text{fold}}$ is only valid for sources sufficiently close to the caustic that higher-order terms are negligible. To quantify this statement, we compare our analytic approximation with the differential time delay computed numerically from the exact form of the lens equation. The numerical analysis requires a specific lens model, so we consider an SIE with axis ratio $q = 0.5$ as a representative example. We use the software of Keeton (2001) to compute the astroid caustic, and then choose a point on the caustic, far from a cusp, to serve as the origin of the (u_1, u_2) frame. For a given value of u_2 , we solve the exact lens equation to obtain the image positions and time delay for the fold doublet. The top left panel of Figure 2 shows $\Delta\hat{\tau}_{\text{fold}}$ in units of θ_E^2 as a function of u_2 in units of θ_E , where θ_E is the Einstein angle of the lens. The analytic and numerical results are in good agreement for sources within $0.05\theta_E$ of the caustic, although the curves do begin to diverge as u_2 increases. The difference between the numerical and analytic curves (which represents the error in the analytic approximation, denoted by ϵ) is shown in the middle left panel. The bottom left panel shows the logarithmic slope of the error curve, $d(\ln \epsilon)/d(\ln u_2)$. Together, the middle and bottom left panels verify that our analytic approximation is accurate at order $\epsilon^{3/2}$. Furthermore, these panels suggest that the next non-vanishing term is of order $\epsilon^{5/2}$ and has a positive coefficient. The interesting implication is that the coefficient of the ϵ^2 term seems to vanish. At our current order of approximation we are not able to determine whether this is rigorously true, and if so, how general it is; we merely offer the remark in the hope that it may be useful for future analytic studies. For now, we focus on the verification that our analytic approximation is accurate at the order to which we work.

Since the source position u_2 is not observable, we compare the analytic and numerical time delays as a function of the image separation d_1 in the right-hand panels of Figure 2. The range of d_1 corresponds to that used for u_2 in the left-hand panels. For a canonical fold lens with $d_1 = 0.46\theta_E$ (Keeton et al. 2005), our analytic expression gives a very good approximation, indicating that our analysis can be applied in astrophysically relevant situations—not just when the source is asymptotically close to the caustic, but even when it lies some small but finite distance away.

4 THE CUSP CASE

We now apply our perturbative method to the case of a source near a cusp point. This approach has not been applied to cusp lenses before. Appendix A of Keeton et al. (2003) derives the image positions and magnifications for a cusp triplet assuming a simplified form of the lens equation. As we noted in Section 1, this simplified lens equation assumes that certain terms may be set to zero, using criteria that are less than rigorous. We use the lens equation derived from the fourth-order lens potential, and use perturbation theory to verify the results of Keeton et al. (2003) and extend the analysis to a higher order of approximation. We also study time delays for a cusp lens for the first time. Our analysis does not involve simplifying assumptions, and indicates that perturbation theory is a powerful method in the study of lensing.

4.1 Image Positions

We again expand the image positions, magnifications and time delays in the parameter ϵ , but with one notable difference. For a cusp oriented in the u_1 direction, a small “horizontal” displacement of ϵu_1 from the cusp point permits a “vertical” displacement of only $\epsilon^{3/2} u_2$ (see Fig. 1), since larger vertical displacements would imply a source position outside the caustic (Blandford & Narayan 1986). The lens equation is then

$$\epsilon u_1 = K\theta_1 - (3e\theta_1^2 + 2f\theta_1\theta_2 + g\theta_2^2) - (4k\theta_1^3 + 3m\theta_1^2\theta_2 + 2n\theta_1\theta_2^2 + p\theta_2^3), \quad (26)$$

$$\epsilon^{3/2} u_2 = -(f\theta_1^2 + 2g\theta_1\theta_2) - (m\theta_1^3 + 2n\theta_1^2\theta_2 + 3p\theta_1\theta_2^2 + 4r\theta_2^3) \quad (27)$$

(see Petters et al. 2001, Theorem 9.1), where the θ_2^2 term of equation (13) does not appear, since $\psi_{222}(0) = 0$ for a cusp, corresponding to $h = 0$ in equation (11).

As before, we write the image positions as a series expansion in ϵ , but now keeping an additional term (i.e., $\gamma_i \epsilon^{3/2}$). This is necessary since the vertical component of the source position enters the lens equation as $\epsilon^{3/2} u_2$, rather than ϵu_2 as in the fold case. We have

$$\theta_1 = \alpha_1 \epsilon^{1/2} + \beta_1 \epsilon + \gamma_1 \epsilon^{3/2} + \mathcal{O}(\epsilon^2), \quad (28)$$

$$\theta_2 = \alpha_2 \epsilon^{1/2} + \beta_2 \epsilon + \gamma_2 \epsilon^{3/2} + \mathcal{O}(\epsilon^2). \quad (29)$$

The lens equation then becomes

$$0 = \alpha_1 K \epsilon^{1/2} - (3e\alpha_1^2 + 2f\alpha_1\alpha_2 + g\alpha_2^2 - \beta_1 K + u_1) \epsilon - [4k\alpha_1^3 + 3m\alpha_1^2\alpha_2 + p\alpha_2^3 + 2\alpha_1(n\alpha_2^2 + 3e\beta_1 + f\beta_2) + 2\alpha_2(f\beta_1 + g\beta_2) - K\gamma_1] \epsilon^{3/2} + \mathcal{O}(\epsilon^2), \quad (30)$$

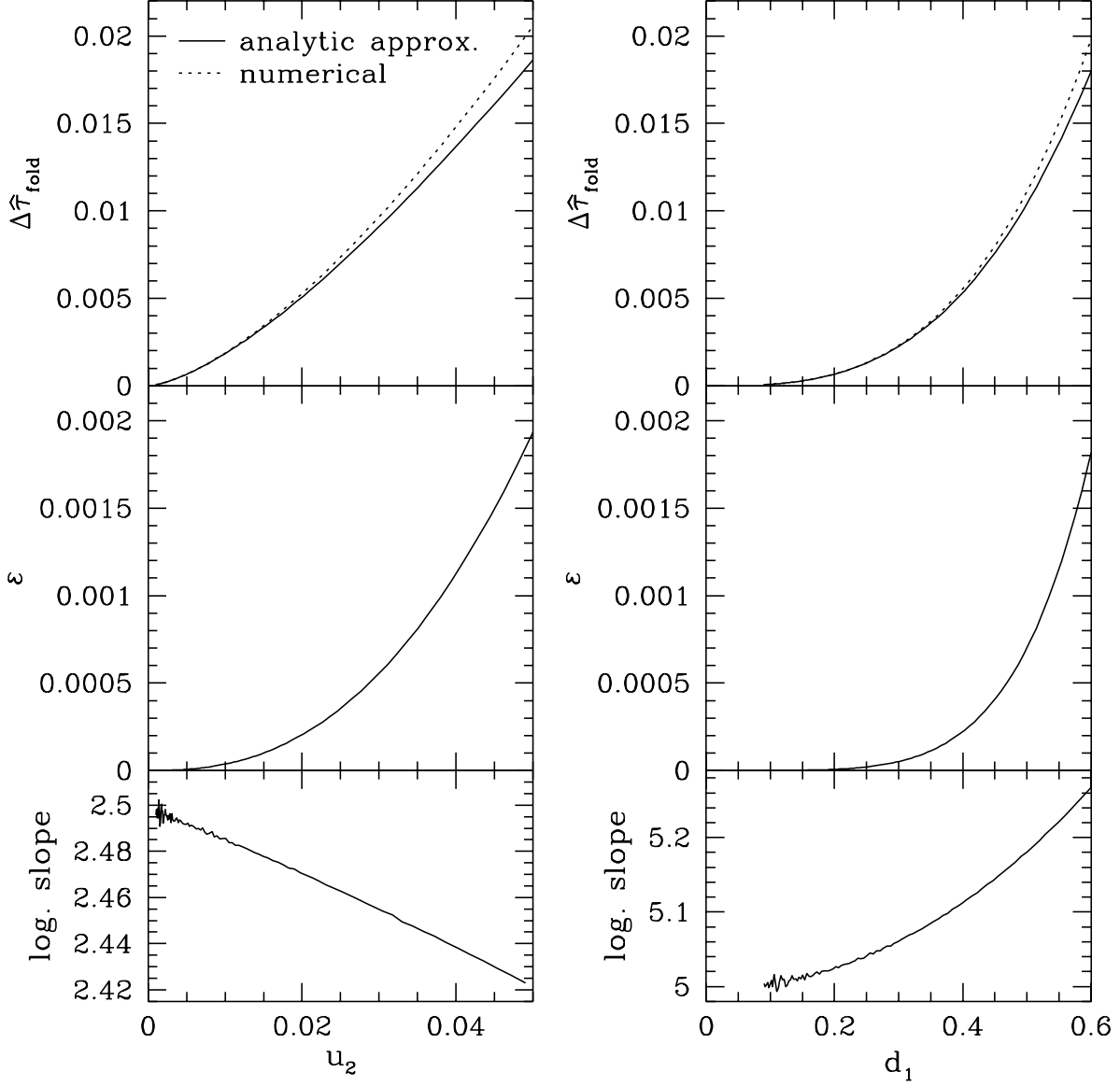


Figure 2. The top panels show the time delay for a fold pair as a function of source position (left) and image separation (right), for an SIE lens with axis ratio $q = 0.5$. The solid line shows our analytic approximation while the dotted line shows the exact result obtained by solving the lens equation numerically. The quantities u_2 and d_1 are defined in the text, and are shown here in units of the Einstein angle, θ_E . The time delay is given in units of θ_E^2 . The middle panels show the error in the analytic approximation, $\epsilon = \Delta\hat{\tau}_{\text{fold}}(\text{numerical}) - \Delta\hat{\tau}_{\text{fold}}(\text{analytic})$, due to our neglect of higher-order terms. The bottom panels show the logarithmic slope of the error curve, $d(\ln \epsilon)/d(\ln u_2)$ on the left and $d(\ln \epsilon)/d(\ln d_1)$ on the right. There is some numerical noise in the logarithmic slope due to numerical differentiation. Together the middle and bottom panels verify that our analytic expression is accurate at order $\epsilon^{3/2}$ (cf. equation 25).

$$\begin{aligned}
 0 = & -(f\alpha_1^2 + 2g\alpha_1\alpha_2)\epsilon - (u_2 + m\alpha_1^3 + 2n\alpha_1^2\alpha_2 + 3p\alpha_1\alpha_2^2 + 4r\alpha_2^3 + 2f\alpha_1\beta_1 + 2g\alpha_2\beta_1 + 2g\alpha_1\beta_2)\epsilon^{3/2} \\
 & - \left\{ \beta_1(f\beta_1 + 2g\beta_2) + \alpha_1^2(3m\beta_1 + 2n\beta_2) + 3\alpha_2^2(p\beta_1 + 4r\beta_2) + 2g\alpha_2\gamma_1 + 2\alpha_1[\alpha_2(2n\beta_1 + 3p\beta_2) + f\gamma_1 + g\gamma_2] \right\} \epsilon^2 \\
 & + \mathcal{O}(\epsilon)^{5/2}.
 \end{aligned} \tag{31}$$

As in the fold case (see equation 16), we find $\alpha_1 = 0$. Note that γ_2 appears only in the ϵ^2 coefficient of equation (31), but in a term multiplied by α_1 . Hence, it will not be possible to solve for γ_2 . Fortunately, it turns out that the expressions we would like to derive do not involve this parameter.

We can now write the lens equation as

$$0 = -(g\alpha_2^2 - \beta_1K + u_1)\epsilon - [p\alpha_2^3 + 2\alpha_2(f\beta_1 + g\beta_2) - K\gamma_1]\epsilon^{3/2} + \mathcal{O}(\epsilon)^2, \tag{32}$$

$$0 = -(u_2 + 4r\alpha_2^3 + 2g\alpha_2\beta_1)\epsilon^{3/2} - [\beta_1(f\beta_1 + 2g\beta_2) + 3\alpha_2^2(p\beta_1 + 4r\beta_2) + 2g\alpha_2\gamma_1]\epsilon^2 + \mathcal{O}(\epsilon)^{5/2}. \quad (33)$$

Recalling that these equations must be satisfied at each order in ϵ , we then solve for the unknown coefficients:

$$\beta_1 = \frac{g\alpha_2^2 + u_1}{K}, \quad (34)$$

$$\beta_2 = -\frac{(5fg^2 + 5gKp)\alpha_2^4 + (6fgu_1 + 3Kpu_1)\alpha_2^2 + fu_1^2}{2K(3g^2\alpha_2^2 + 6Kr\alpha_2^2 + gu_1)}, \quad (35)$$

$$\gamma_1 = \frac{(fg^3 - 2g^2Kp + 12fgKr + 6K^2pr)\alpha_2^5 + (2fg^2u_1 - 2gKpu_1 + 12fKru_1)\alpha_2^3 + fg u_1^2 \alpha_2}{K^2(3g^2\alpha_2^2 + 6Kr\alpha_2^2 + gu_1)}, \quad (36)$$

where α_2 satisfies the cubic equation

$$\alpha_2^3 + \frac{gu_1}{2Kr + g^2}\alpha_2 + \frac{Ku_2}{4Kr + 2g^2} = 0. \quad (37)$$

This is equivalent to equation (A8) from Keeton et al. (2003), after making the replacements $\alpha_2 \rightarrow z$, $K \rightarrow c$, $g \rightarrow -b/2$, $r \rightarrow -a/4$. To leading order, the image positions can be written as

$$\theta_1 = \beta_1\epsilon = \frac{g\alpha_2^2 + u_1}{K}\epsilon, \quad (38)$$

$$\theta_2 = \alpha_2\epsilon^{1/2}, \quad (39)$$

which are equivalent to equation (A7) from Keeton et al. (2003). The distance between any two images i and j is then

$$d_{ij} = [\alpha_2^{(i)} - \alpha_2^{(j)}]\epsilon^{1/2} + \mathcal{O}(\epsilon). \quad (40)$$

4.2 Magnifications

Substituting our perturbative expressions for the image positions into equation (8), we find that the inverse magnification of a cusp image is given by:

$$\mu^{-1} = -2[gu_1 + 3(g^2 + 2Kr)\alpha_2^2]\epsilon + [(24fr - 12gp)\alpha_2^3 + (6Kp - 4fg)\alpha_2\beta_1 - (8g^2 + 24Kr)\alpha_2\beta_2 - gK\gamma_1]\epsilon^{3/2} + \mathcal{O}(\epsilon)^2. \quad (41)$$

We then find from equation (2) that

$$R_{\text{cusp}} = 0 + \mathcal{O}(\epsilon) \approx A_{\text{cusp}}d^2, \quad (42)$$

where $d = \max_{ij} d_{ij}$ is the largest separation between any two of the three cusp images. This expression shows that correction terms to the ideal cusp relation enter at second order in the image separation, which agrees with the conjecture of Keeton et al. (2003). To see this, we define $m_i \equiv |\mu_i^{-1}|$, which allows us to write

$$R_{\text{cusp}} = \frac{m_B m_C - m_A m_C + m_A m_B}{m_B m_C + m_A m_C + m_A m_B}. \quad (43)$$

If the leading-order term in the numerator vanishes, so does the leading-order term in R_{cusp} . The zeroth-order term in R_{cusp} corresponds to a term of $\mathcal{O}(\epsilon)^2$ in the numerator, since the leading-order term in the denominator is $\mathcal{O}(\epsilon)^2$. By substituting the solutions for α_2 into the numerator, we find that $R_{\text{cusp}} = 0$ to lowest order, in agreement with Keeton et al. (2003). We repeat this procedure for the next-leading term of $\mathcal{O}(\epsilon)^{5/2}$ in the numerator, and find that $R_{\text{cusp}} = 0$ at linear order in d [i.e., $\mathcal{O}(\epsilon)^{1/2}$] as well; this result was unattainable using the formalism of Keeton et al. (2003). To proceed to higher order, we must extend our perturbative analysis by including terms of the form $\delta_i\epsilon^2$ in equations (28) and (29) for the image positions. We denote the coefficient of d^2 by A_{cusp} , which we do not here write down, since that would require several pages. Given the complexity of this term, it is not practical to evaluate A_{cusp} analytically. However, we have numerically computed R_{cusp} for the case of an SIE model with $q = 0.5$ (see Fig. 3) and find that $R_{\text{cusp}} \propto u_1 \propto d^2$. While it is conceivable that A_{cusp} might be zero for some specific lens model, clearly this is not the case in general. We have thus demonstrated analytically that R_{cusp} vanishes through linear order in d , placing the numerical result of Keeton et al. (2003) on solid mathematical ground.

4.3 Time Delays

For the cusp case, the scaled time delay takes the form

$$\hat{\tau} = \frac{1}{2} [(\theta_1 - \epsilon u_1)^2 + (\theta_2 - \epsilon^{3/2} u_2)^2] - \psi(\theta_1, \theta_2). \quad (44)$$

We find

$$\hat{\tau} = \frac{1}{2K} [(3g^2 + 6Kr)\alpha_2^4 + 2gu_1\alpha_2^2 + (K - 1)u_1^2]\epsilon^2 + \mathcal{O}(\epsilon)^{5/2}, \quad (45)$$

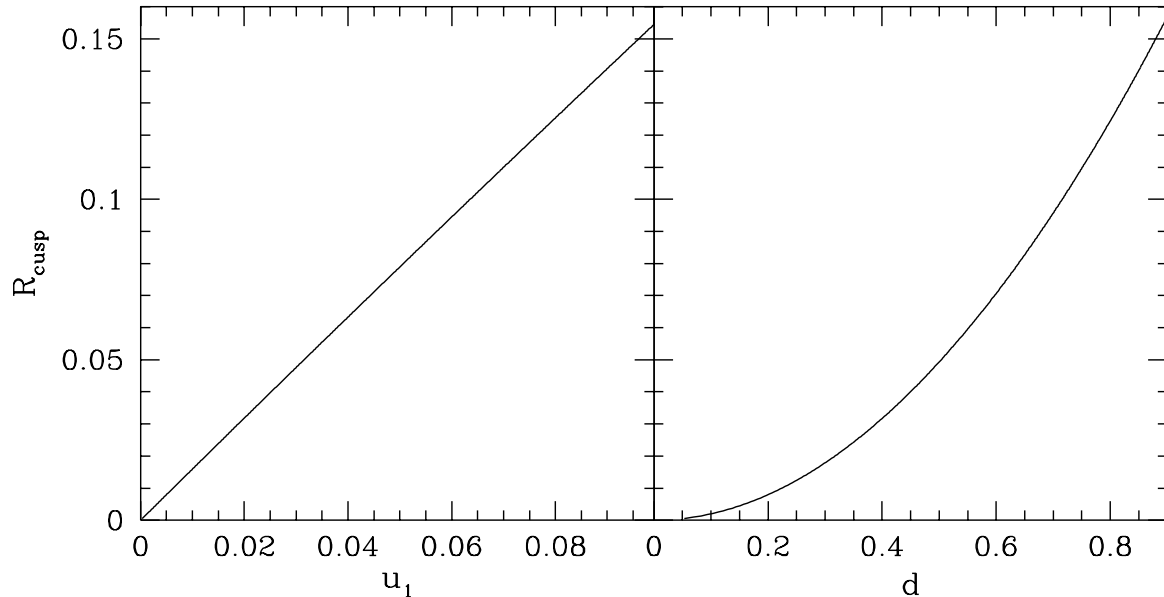


Figure 3. R_{cusp} as a function of u_1 (left) and d (right) for an SIE with $q = 0.5$, obtained by solving the lens equation numerically.

corresponding to a differential time delay of

$$\Delta \hat{\tau}_{\text{cusp}}^{(ij)} = \frac{1}{4K} \left[2g \left(\alpha_2^{(i)} + \alpha_2^{(j)} \right) u_1 + 3K u_2 \right] \left(\alpha_2^{(j)} - \alpha_2^{(i)} \right) \epsilon^2. \quad (46)$$

Unlike the fold case, the time delay for a pair of cusp images depends on both source coordinates (u_1, u_2) . This means that it is not possible to write our current expression strictly in terms of observables, such as the image separation. Instead, all we can say is that the time delay scales quadratically with ϵ , or alternatively, with the fourth power of the image separation.

In the fold case, we found that the time delay scales as $\epsilon^{3/2}$ and only depends on the lens potential through the parameter h . For a cusp, however, $h = 0$, so it is not surprising that the lowest-order term in the time delay is of $\mathcal{O}(\epsilon)^2$. Furthermore, if we had not included the $\gamma_i \epsilon^{3/2}$ terms in our expansions of the image positions for a cusp [equations (28) and (29)], it would not have been possible to obtain a perturbative expression for the time delay; instead, we would simply have found $\hat{\tau} = 0 + \mathcal{O}(\epsilon)^2$.

5 SUMMARY

We have developed a unified, rigorous framework for studying lensing near fold and cusp critical points, which can (in principle) be extended to arbitrary order. We have found that the differential time delay of a fold pair assumes a particularly simple form, depending only on the image separation and the Taylor coefficient $h = \psi_{222}(0)/6$. This result is astrophysically relevant, since it is quite accurate even for sources that are not asymptotically close to the caustic. We have also obtained perturbative expressions for the image positions, magnifications and time delays of a cusp triplet. These results rest on the key insight that a source at a given distance ϵ from a cusp along the relevant symmetry axis of the caustic can only move a perpendicular distance of $\epsilon^{3/2}$ in order to remain inside the caustic (Blandford & Narayan 1986). We have shown rigorously that the distance dependence of the magnification ratio R_{cusp} conjectured by Keeton et al. (2003) is correct. We have also demonstrated that the leading-order expression for the image positions is given by the relations presented by Keeton et al. (2003), and have provided the necessary framework for deriving the image positions corresponding to a Taylor expansion of the lens potential at arbitrary truncation order. Finally, we have derived cusp time delays analytically for the first time. Our results provide a rigorous foundation for identifying anomalous flux ratios and time delays in gravitational lens systems, and for using them to study small-scale structure in the mass distributions of distant galaxies.

ACKNOWLEDGMENTS

We thank A. O. Petters and Peter Schneider for helpful discussions and suggestions, and for their careful reading of the manuscript. We also thank the anonymous referee for useful comments.

REFERENCES

- Bellman, R. 1966, *Perturbation Techniques in Mathematics, Engineering, and Physics* (Mineola, NY: Dover)
- Blandford, R., & Narayan, R. 1986, *ApJ*, 310, 568
- Chiba, M. 2002, *ApJ*, 565, 17, arXiv:astro-ph/0109499
- Congdon, A. B., & Keeton, C. R. 2005, *MNRAS*, 364, 1459, arXiv:astro-ph/0510232
- Dalal, N., & Kochanek, C. S. 2002, *ApJ*, 572, 25, arXiv:astro-ph/0111456
- Diemand, J., Kuhlen, M., & Madau, P. 2007, *ApJ*, 657, 262
- Dobler, G., & Keeton, C. R. 2006, *MNRAS*, 365, 1243, arXiv:astro-ph/0502436
- Evans, N. W., & Witt, H. J. 2003, *MNRAS*, 345, 1351, arXiv:astro-ph/0212013
- Falco, E. E., Lehar, J., & Shapiro, I. I. 1997, *AJ*, 113, 540, arXiv:astro-ph/9612182
- Gao, L., White, S. D. M., Jenkins, A., Stoehr, F., & Springel, V. 2004, *MNRAS*, 355, 819
- Gaudi, B. S., & Petters, A. O. 2002a, *ApJ*, 574, 970, arXiv:astro-ph/0112531
- . 2002b, *ApJ*, 580, 468, arXiv:astro-ph/0206162
- Hogg, D. W., & Blandford, R. D. 1994, *MNRAS*, 268, 889, arXiv:astro-ph/9311077
- Keeton, C. R. 2001, astro-ph/0102340
- Keeton, C. R., Gaudi, B. S., & Petters, A. O. 2003, *ApJ*, 598, 138, arXiv:astro-ph/0210318
- . 2005, *ApJ*, 635, 35, arXiv:astro-ph/0503452
- Keeton, C. R., Kochanek, C. S., & Seljak, U. 1997, *ApJ*, 482, 604, arXiv:astro-ph/9610163
- Keeton, C. R., & Moustakas, L. A. 2008, arXiv:0805.0309, 805
- Klypin, A., Kravtsov, A. V., Valenzuela, O., & Prada, F. 1999, *ApJ*, 522, 82, arXiv:astro-ph/9901240
- Koopmans, L. V. E., Treu, T., Bolton, A. S., Burles, S., & Moustakas, L. A. 2006, *ApJ*, 649, 599, arXiv:astro-ph/0601628
- Kormann, R., Schneider, P., & Bartelmann, M. 1994, *A&A*, 284, 285
- Mao, S. 1992, *ApJ*, 389, 63
- Mao, S., Jing, Y., Ostriker, J. P., & Weller, J. 2004, *ApJ*, 604, L5
- Mao, S., & Schneider, P. 1998, *MNRAS*, 295, 587, arXiv:astro-ph/9707187
- McKean, J. P. et al. 2007, *MNRAS*, 378, 109
- Metcalf, R. B., & Madau, P. 2001, *ApJ*, 563, 9
- Moore, B., Ghigna, S., Governato, F., Lake, G., Quinn, T., Stadel, J., & Tozzi, P. 1999, *ApJ*, 524, L19, arXiv:astro-ph/9907411
- Petters, A. O., Levine, H., & Wambsganss, J. 2001, *Singularity Theory and Gravitational Lensing* (Boston: Birkhäuser)
- Rusin, D., & Kochanek, C. S. 2005, *ApJ*, 623, 666, arXiv:astro-ph/0412001
- Schechter, P. L., & Moore, C. B. 1993, *AJ*, 105, 1
- Schneider, P., Ehlers, J., & Falco, E. E. 1992, *Gravitational Lenses* (Berlin: Springer-Verlag)
- Schneider, P., & Weiss, A. 1992, *A&A*, 260, 1
- Strigari, L. E., Bullock, J. S., Kaplinghat, M., Diemand, J., Kuhlen, M., & Madau, P. 2007, *ApJ*, 669, 676, arXiv:0704.1817
- Yoo, J., Kochanek, C. S., Falco, E. E., & McLeod, B. A. 2005, *ApJ*, 626, 51, arXiv:astro-ph/0502299
- . 2006, *ApJ*, 642, 22, arXiv:astro-ph/0511001
- Zakharov, A. F. 1995, *A&A*, 293, 1